Journal of Catalysis **189,** 105–116 (2000)
doi:10.1006/jcat.1999.2688, available online at http://www.idealibrary.com on IDEAL®

Alumina-Supported Copper Chloride

2. Effect of Aging and Thermal Treatments

G. Leofanti,*,[1] M. Padovan,*,[2] M. Garilli,* D. Carmello,* G. L. Marra,† A. Zecchina,‡ G. Spoto,‡ S. Bordiga,‡ and C. Lamberti‡,§,[3]

*Inovyl Technological Centre, European Vinyls Corporation Italia, Via della Chimica 5, 30175 Porto Marghera, Venezia, Italy; †EniChem S. p. A., Centro Ricerche Novara, Instituto Guido Donegani, Via G. Fauser 4, I-28100 Novara, Italy; ‡Dipartimento di Chimica Inorganica, Chimica Fisica e Chimica dei Materiali, Università di Torino, Via P. Giuria 7, 10125 Torino, Italy; and §INFM Setione di Torino

Received June 4, 1999; revised September 1, 1999; accepted September 3, 1999

The effect of aging and heating treatments up to 500 K on alumina-supported $CuCl_2$, i.e., the base catalyst for ethylene oxychlorination, has been investigated by UV–vis spectroscopy, a solubility test, EXAFS, XRD, and EPR in a wide range (0.25–9 wt%) of Cu concentration. It is shown that the catalyst undergoes significant changes with both time and thermal treatments, so accounting for some contradictory results reported in the literature. While the surface Cu aluminate (formed during impregnation) does not change upon aging and heating, supported $CuCl_2$ (precipitated from impregnating solution during the drying process) undergoes a slow hydrolysis reaction with the formation of paratacamite and HCl. The HCl formed during the hydrolysis reacts with the alumina surface with the formation of >Al–Cl species. Upon heating, the initially formed paratacamite can react with surface >Al–Cl species with nearly total restoration of $CuCl_2$, which is consequently the main species present on the catalyst at the beginning of the oxychlorination reaction. The obtained picture is able to explain the results emerging from activity tests on the whole set of catalysts, indicating that surface aluminate is not active and that the active phase is $CuCl_2$. © 2000 Academic Press

Key Words: **Al_2O_3-supported $CuCl_2$; ethylene oxychlorination; EXAFS; copper solubility.**

1. INTRODUCTION

This paper represents the second part of a series devoted to the investigation of $CuCl_2$ supported on γ-alumina, the base catalyst for ethylene oxychlorination. The aim of the whole work is (i) to identify the species present at different Cu loadings, (ii) to determinate their concentration, and (iii) to investigate the possibility of mutual transformations during impregnation, aging, and heating treatments up to the typical oxychlorination temperature (500–550 K). In the first paper (1), beside a brief overview of the available literature data, the species present on fresh catalysts with the Cu concentration ranging from 0.25 to 9.0 wt% were investigated, by means of UV–vis spectroscopy, solubility tests, EPR, EXAFS, and XRD. The samples were examined immediately after impregnation (practically after a short and mild drying process) to minimize the reactions associated with aging and heating. From this first study (1) it has been concluded that (i) at copper content lower than 0.95 wt% Cu/100 m^2 of support, the formation of surface aluminate takes place where the copper ions are surrounded by oxygen ligands which only form a tetragonally distorted octahedral environment; (ii) the chlorine released by $CuCl_2$ during its interaction with alumina gives surface >Al–Cl species; (iii) once the adsorptive capacity of alumina is exhausted (which occurs for copper content greater than 0.95 wt% Cu/100 m^2 of support), copper chloride precipitates directly from the solution with the formation of $CuCl_2 \cdot 2H_2O$; (iv) simultaneously a slow hydrolysis process takes place with the formation of a small concentration of copper hydroxochloride (paratacamite).

In this second paper we discuss the effect of aging and heating on the structure of the surface species discussed above. We will show that the catalyst undergoes significant changes with time and temperature. In particular, it will be apparent that aging at room temperature (RT) can play a significant role in determining the structure and the properties of the supported species and that this effect can account for some contradictory results reported in the literature, as discussed in Ref. (1).

2. EXPERIMENTAL

2.1. Materials

To follow the structural transformations of copper species induced by aging, six samples with a Cu loading ranging from 0.25 to 9.0 wt% (prepared as extensively reported in the previous paper (1)), have been characterized with

[1] Present address: Via Firenze 43, 20010 Canegrate, Milano, Italy.
[2] Present address: Via Villa Mirabello 1, 20125 Milano, Italy.
[3] To whom correspondence should be addressed. E-mail: Lamberti@ch.unito.it (internet). Fax: +39-011-6707855.

0021-9517/00 $35.00
Copyright © 2000 by Academic Press
All rights of reproduction in any form reserved.

various independent techniques (see below) after 1 day and 6 months since impregnation. Comparison is made with results obtained on the as prepared samples, already discussed in paper (1). The 6-month aged samples were also examined after drying *in vacuo* up to 623 K, to cover a typical oxychlorination temperature range (500–550 K). To help the interpretation of the results, a few samples treated in different conditions were also studied: $CuCl_2 \cdot 2H_2O$, CuO, Cu_2O, CuCl, $CuCl_2$, $Cu_2(OH)_3Cl$, CuO0.5, and CuO0.25, obtained as reported in (1), were used as reference compounds.

2.2. Methods

Elemental analysis, solubility tests, UV–vis, EXAFS, EPR, and RT XRD techniques have been used to characterize the samples reported in Ref. (1); we shall therefore refer to Section 2.2. of that paper for any technical detail.

High-temperature XRD patterns have been collected in the 300–493 K interval over the 5°–50° 2θ range by means of a Philips 1050/25 $\theta/2\theta$ diffractometer, equipped with a Anton Paar HTK 10 high-temperature chamber. The final temperature (493 K) was obtained by raising T with a speed of 5 K min^{-1}, and three intermediate stops at 328, 383, and 438 K. Ni-filtered Cu$K\alpha$ radiation at 40 kV with a 30-mA current has been used.

Activity tests of the oxychlorination reaction have been made by using a conventional pulse reactor with the following procedure. The reactor, containing 0.15 g of sample, was heated to 500 K in a nitrogen stream (30 cm^3 min^{-1}). To ensure a complete and stable re-chlorination of the catalyst, the sample was then treated with alternate pulses of air (0.75 cm^3) and HCl (0.60 cm^3) five times; a series of C_2H_4 pulses (0.30 cm^3) were then sent to the sample and the C_2H_4-to-$C_2H_4Cl_2$ conversion has been determined by a gas chromatograph (Carlo Erba Fractovap 4200) equipped with a packed column, a flame detector, and an integrator (Shimadzu C-R3A Chromatopac). The side products usually found in tests on oxychlorination reaction (for example, ethyl chloride and vinyl chloride) have been not detected in our experiments, probably because of the adopted depletion procedure.

3. RESULTS AND DISCUSSION

Starting from the results of previous work on fresh samples (1), in the following two sections we deal with the effect of aging and of heating, while in the third we will comment on the results of the activity tests in ethylene oxychlorination on the basis of what evidenced in the first paper (1) and in the two previous sections of this paper.

3.1. Effect of Aging on the Structure of the Supported Species

The physical and chemical properties of low copper-concentrated samples (up to Cu1.4) do not change with aging time. In other words, the surface aluminate is stable. In fact, the comparison of the UV–vis spectra measured on the Cu0.25 freshly prepared samples and after 1-day and 6-month aging (Fig. 1) demonstrates that the Cu–aluminate surface phase, dominating in the low-concentrated samples, is not affected by aging time. This behavior agrees with the stability of the surface aluminate under heating at 923 K (anticipated in Fig. 2a of Ref. (1) and related discussion). The same behavior is observed in the UV–vis spectra of Cu0.5 and Cu1.4 samples (not reported here for sake of brevity). This conclusion is confirmed by a solubility test which shows no evidence of appreciable change with time, being the copper of all low-loaded samples (fresh and aged) completely insoluble in ethyl alcohol. Also, EPR spectra of samples Cu0.035, Cu0.25, Cu0.5, and Cu1.4, measured after 1 day and 6 months (not reported for brevity) do not show significant differences with respect to the corresponding spectra measured after 1 h from impregnation and reported in Fig. 4a of paper (1).

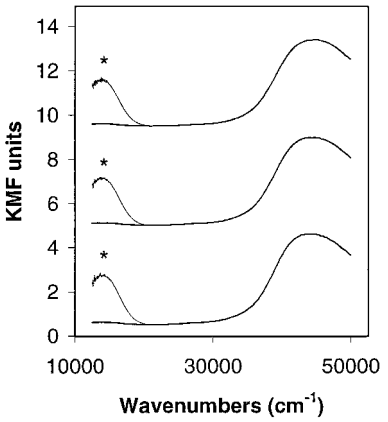

FIG. 1. UV–vis DRS spectra of the Cu0.25 sample at increasing aging time. From top to bottom: 1 h, 1 day, and 6 m. The *d–d* transition band has been magnificated by a factor of 20 in the 12,500- to 20,000-cm^{-1} range to appreciate its substantial invariance upon aging (see stars).

On the contrary, UV–vis spectra of high-concentrated samples show that, during aging at RT, a consistent transformation of the sample structure is occurring. In particular, in Fig. 2 the spectra of the Cu9.0 sample, either fresh or after increased aging time are reported and compared with those of hydrated $CuCl_2$ and $Cu_2(OH)_3Cl$ (paratacamite) model compounds. Comparison with the spectra of hydrated $CuCl_2$ is necessary because the results of Ref. (1) have evidenced that it represents the main copper phase present on as-prepared samples with high-Cu content. Comparison with paratacamite is also made because its formation on aged samples has been determined by XRD (*vide infra*). The most relevant spectral modifications induced by aging can be summarized as follows: (i) the intensity of the *d–d* transition band undergoes a strong decrease; (ii) the component at 40,000–43,000 cm^{-1}

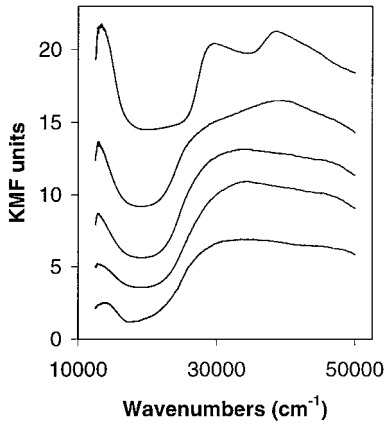

FIG. 2. UV–vis DRS spectra of Cu9.0 sample at increasing aging time compared with those of hydrated copper chloride and paratacamite model compounds. From top to bottom: $CuCl_2 \cdot 2H_2O$, Cu9.0 sample after 1 h, 1 day, and 6 months and $Cu_2(OH)_3Cl$.

in the CT region, clearly visible in the as-prepared sample, disappears upon aging, resulting in a nearly flat absorption for $\nu > 30{,}000$ cm^{-1}. The comparison with the spectra of model compounds clearly indicates that aging induces a progressive evolution from a spectrum similar to that of hydrated $CuCl_2$ (upper spectrum in Fig. 2) toward a paratacamite-like spectrum (lower spectrum in Fig. 2). This evolution, which is not associated with the loss of chlorine (as pointed out by the elemental analysis), is progressive and regards all the samples containing copper chloride, as pointed out in Fig. 3, where the *d–d* band intensity is reported as a function of the aging time. The gradual decrement of the *d–d* band intensity is the expected result of the transformation of $CuCl_2 \cdot 2H_2O$ into paratacamite, because the extinction coefficient of hydrated $CuCl_2$ is larger than that of paratacamite due to a higher chemical heterogeneity in the ligands of the first coordination sphere around Cu(II). In fact, while the nearest local structure around copper ion

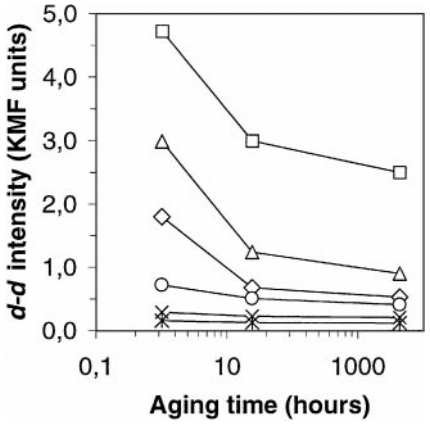

FIG. 3. Effect of aging time on *d–d* transition band intensity. From top to bottom: Cu9.0 (□), Cu4.6 (△), Cu2.3 (◇), Cu1.4 (○), Cu0.5 (×), and Cu0.25 (*).

in hydrated $CuCl_2$ is consisting of 2 oxygen atoms at 1.95 Å and two chlorines at 2.29 Å (2), paratacamite has 2 equipopulated copper sites, the former being a regular octahedron with 6 oxygen ligands at 2.11 Å and the latter being an elongated octahedron with 4 planar oxygen ligands at 1.98 Å and 2 axial chlorine ligands at 2.78 Å (3). Thevspace*.2pt effect of the insertion of the chlorine atoms in the coordination sphere of Cu(II) on the *d–d* band intensity is weaker in paratacamite than in hydrated copper chloridevspace*.2pt due to the fact that only a fraction of Cu(II) exhibits a chemical heterogeneity in the ligand sphere and to the fact that, in that case, the Cu–Cl distance is much higher (2.78 vs 2.29 Å). The gradual disappearance of the copper chloride phase cannot be monitored by XRD since no diffraction lines due to copper chloride have been observed in the patterns of all fresh and aged samples. In section 3.3 of Ref. (1) we have already discussed the reasons why the highly dispersed copper chloride supported phase has no long-range ordering and is XRD-silent. On the contrary, XRD shows the formation of paratacamite (Fig. 4a). By a comparison of the intensity of the paratacamite peak at $2\theta = 16.2^\circ$ measured in the diffraction patterns of the Cu9.0 sample after 1 h, 1 day, and 6 months since impregnation (Fig. 4b), its progressive formation with time is evident. This trend is opposite to what is illustrated in Fig. 3, already attributed to the disappearance of copper chloride.

The main conclusions emerging from the XRD study on the 6-month aged samples (summarized in Fig. 4c, where the intensity of the $2\theta = 16.2^\circ$ peak is reported) are: (i) the diffraction lines of paratacamite are absent in the spectra of low-concentrated samples (0.25–1.4 wt%) and very evident in the spectra of high-loaded ones (2.3–9.0 wt%) and (ii) in the latter set of samples the intensity of paratacamite lines increases with increasing copper concentration. The appearance of paratacamite only on samples with high-Cu content (i.e., only on samples containing copper chloride after impregnation) and the correlation between paratacamite formation and initial copper chloride content point out again that, during the aging process, a slow transformation of $CuCl_2 \cdot 2H_2O$ into $Cu_2(OH)_3Cl$ is occurring. Obviously, low-copper-concentration samples are not involved in this process, reflecting the high stability of the surface copper aluminate.

An evolution with time has also been observed by EPR (first three curves from the top in Fig. 5) where a progressive gain in resolution is observed upon aging. This reflects the evolution from amorphous, highly dispersed $CuCl_2 \cdot 2H_2O$ to crystalline paratacamite, i.e., the evolution from a strong heterogeneous Cu(II) environment to a much more homogeneous one.

The above picture is further supported by the results obtained from a solubility test in ethyl alcohol (Fig. 6), which allows to measure quantitatively the copper chloride content of each sample (1, 4–7). The results reported in

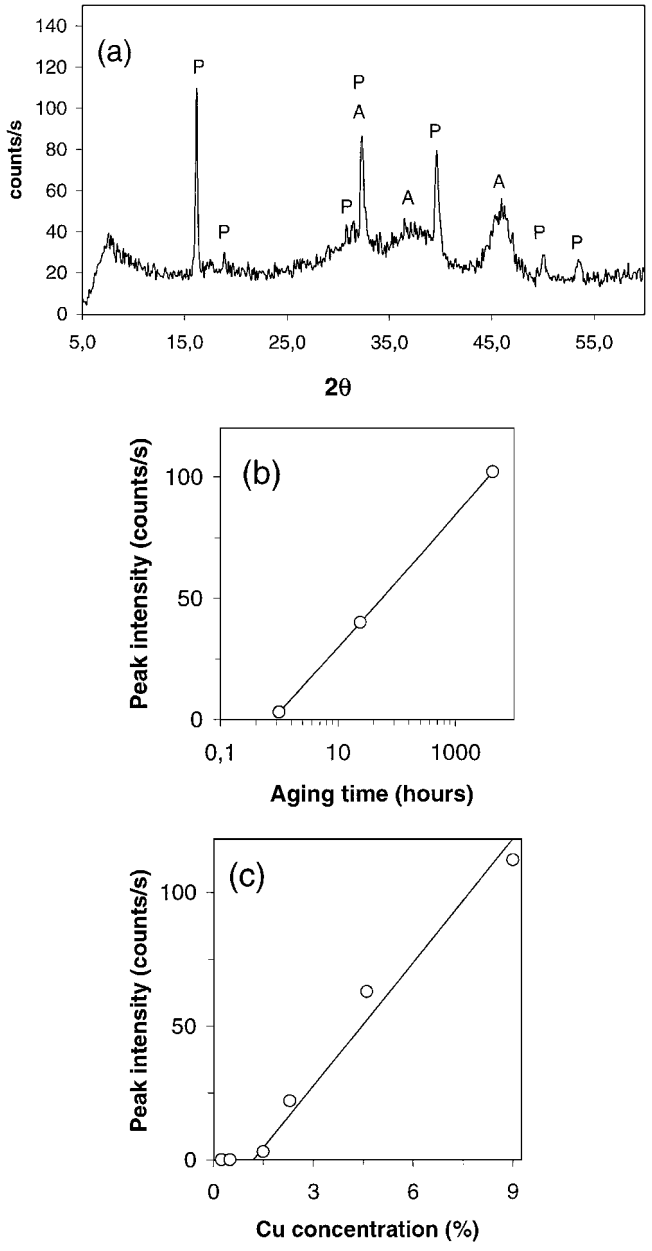

FIG. 4. Part (a): XRD pattern of Cu9.0 sample since 6 months after impregnation. Main diffraction lines due to paratacamite and γ-Al_2O_3 are labeled with P and A, respectively. Part (b): evolution of the intensity of the $2\theta = 16.2^\circ$ paratacamite peak on the Cu9.0 sample as a function of the aging time. Part (c): intensity of the $2\theta = 16.2^\circ$ paratacamite peak on the whole set of the 6-month aged samples.

Fig. 6 can be summarized as follows: (i) the solubility of Cu in the high copper-loaded samples (2.3–9.0 wt%) decreases with the aging time; (ii) for a given aging time the fraction of soluble copper increases (linearly, as will be shown later) with the total copper content. Obviously, in the low-concentrated samples (0.25–1.4 wt%) copper is totally insoluble, independent of the aging time and Cu concentration.

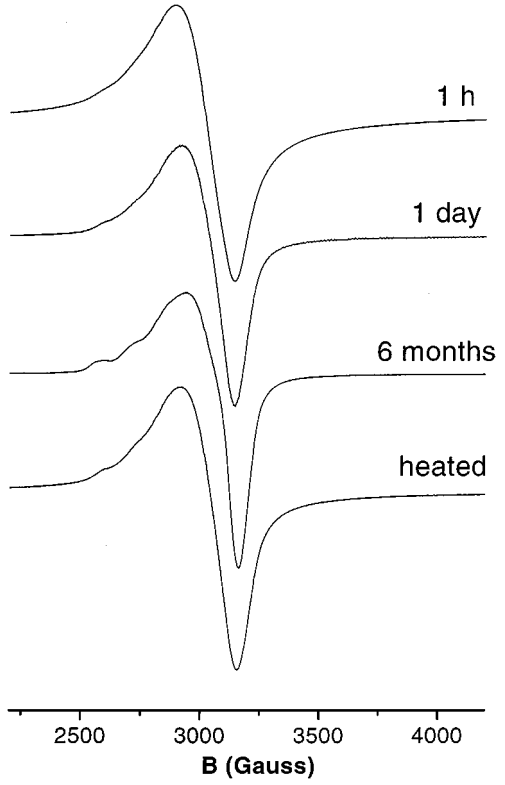

FIG. 5. The first three ERP spectra from top report the effect of aging time on Cu4.6 sample (1 h, 1 day, and 6 month), while the bottom spectrum shows the effect of heating on the 6-month aged sample.

The resulting picture is further confirmed by the conclusion illustrated in Fig. 7. In fact, due to aging, the decrease of both the intensity of the *d–d* transition band and of the soluble copper percentage is correlated to the intensity increase of diffraction lines of paratacamite. Taking into account the relevant quantitative limitation of our UV–vis DRS and XRD data, the relationships shown in Fig. 7 appear to be

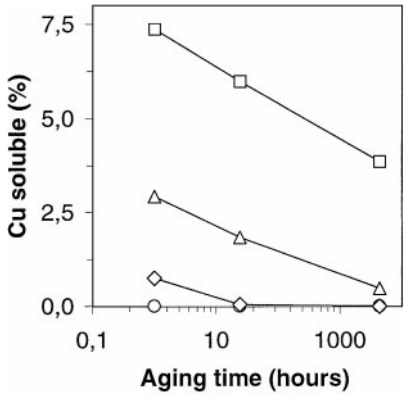

FIG. 6. Effect of aging time on copper solubility. From top to bottom: Cu9.0 (□), Cu4.6 (△), Cu2.3 (◇), and Cu1.4 (○). Data of samples Cu0.5 and Cu0.25 are not reported since totally superimposed to those of sample Cu1.4, reflecting a null solubility.

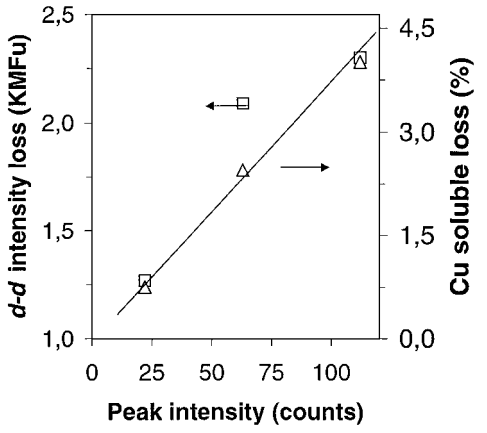

FIG. 7. Evolution of the loss of both *d–d* band intensity (left ordinate scale) and Cu solubility (right ordinate scale) vs the 16.2° 2θ peak intensity.

rather good. This means that the use of solubility data to obtain a quantitative picture of the solid is substantially correct.

The *k*-weighted EXAFS functions (averaged over 5, 3, and 3 spectra, respectively; see Section 2.2 of Ref. (1)) of samples Cu1.4, Cu2.3, and Cu9.0 after 6 months of aging are reported in Fig. 8a (first 3 spectra from the top). As far as sample Cu1.4 is concerned (first spectrum from the top), the absence of any beat in this function suggests that the main contribution to the overall signal comes only from the first coordination shell of the copper absorbers. On the contrary, the sample Cu9.0 (3rd spectrum from the top) shows a strong interference in the 7.5- to 13-$Å^{-1}$ range, indicating that several shells contribute to the overall EXAFS signal. Sample Cu2.3 is in an intermediate situation, being closer to Cu1.4. Corresponding k^3-weighted Fourier transform (FT) reported in Fig. 8b, without any phase correction, reflects, in *R* space, the above-mentioned picture. For comparison, vertically shifted, also the k^3-weighted FT of the $\chi(k)$ of hydrated $CuCl_2$ is reported. At low *R* values this spectrum is dominated by 2 peaks (at 1.49 and 1.94 Å without phase correction) due to 2 oxygens at 1.95 Å and 2 chlorines at 2.29 Å as planar ligands; 2 axial oxygens located at about 4 Å complete the highly distorted octahedral coordination of copper in this compound (2).

Sample Cu1.4 (dotted spectrum) shows only a single peak in the region of Cu–O distances (1.53 Å): no significant

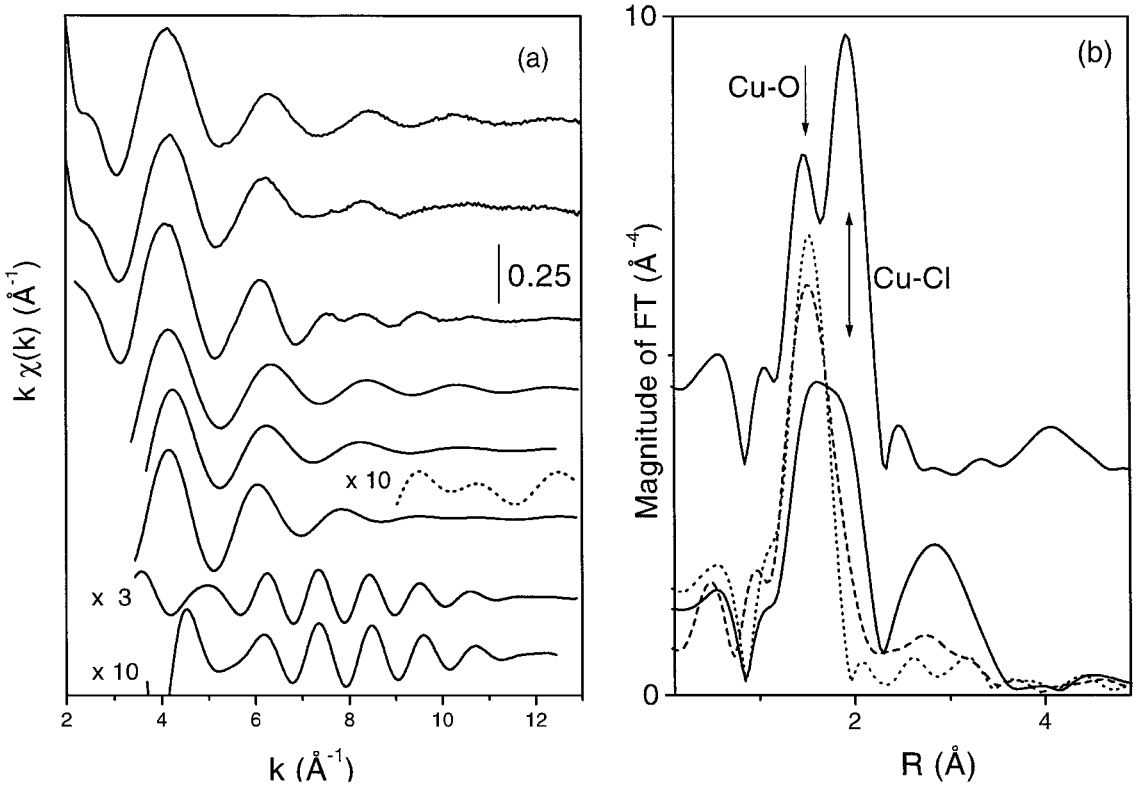

FIG. 8. Part (a) reports in *k*-space the raw EXAFS functions of Cu1.4, Cu2.3, and Cu9.0 samples (first three spectra from top), the corresponding first shell filtered signals (spectra 4, 5, and 6 from top), the second shell filtered signals of samples Cu2.3 (first spectrum from bottom multiplied by a factor of 10) and Cu9.0 (second spectrum from bottom multiplied by a factor of 3). Dotted line spectrum reports, multiplied by a factor of 10, the high *k*-region of first shell filtered signal of sample Cu9.0. Part (b) reports the phase-uncorrected, k^3-weighted FT of the raw EXAFS signals reported in part (a): dotted-, dashed-, and full-line curves for samples Cu1.4, Cu2.3, and Cu9.0, respectively. The vertically shifted full-line spectrum reports the corresponding FT function for the hydrated copper chloride model compound. Vertical arrows indicate where typical Cu–O and Cu–Cl first shell distances are expected in the phase-uncorrected FT functions.

contribution emerges above the noise level from the second shell environment, implying a considerable static disorder or heterogeneity of second shell neighbors around copper. Quantitative EXAFS data analysis gives rise to $N = 4.8(\pm 0.5)$ and $r(\text{Cu-O}) = 1.92(\pm 0.02)$ Å, as already discussed in Ref. (1), and interpreted on the basis of a dispersed surface aluminate phase. On the contrary, Cu9.0 (full-line spectrum) exhibits a much broader first shell peak, clearly shifted at higher R values (maximum at 1.63 Å and shoulder at 1.85 Å), indicating a coexistence of both Cu–O and Cu–Cl contributions. A relevant second shell peak (maximum at 2.85 Å) is also evident. From none of these two shell contributions quantitative EXAFS results can be safely extracted because in both cases we are dealing with overlapped signals coming from different scattering atoms located at different distances in three different phases (surface aluminate, $CuCl_2 \cdot 2H_2O$, and paratacamite). This means that the broad first shell peak extending in the 0.82- to 2.30-Å phase uncorrected range, receives contribution from oxygen atoms of the surface aluminate, at 1.92 Å (1), of the paratacamite at 1.98 and 2.11 Å (3), and of hydrated copper chloride at 1.95 Å, where also chlorine atoms at 2.29 Å are present (2). Since all those Cu–O and Cu–Cl contributions are supposed to have different Debye–Waller factors, the total number of parameters to be optimized in the EXAFS fit becomes too large. This heterogeneity is well-reflected in the first shell filtered signal reported in Fig. 8a, sixth spectrum from top, where heterogeneity completely kills the EXAFS oscillations for $k > 8$ Å^{-1} (the corresponding 10-times magnified dotted-line spectrum shows the high k region of this FT filtered $k\chi(k)$ function). Heterogeneity is also present in the second shell contribution FT filtered in the 2.30- to 3.65-Å region (see the seventh spectrum from top, 3-times magnified, in Fig. 8a), where signals of different frequencies are clearly present. This reflects the fact that Cu in paratacamite has chlorine atoms at 2.78 Å and exhibits two different Cu–Cu distances at 3.06 and 3.41 Å (3). It is worth noticing that no relevant contribution comes from $CuCl_2 \cdot 2H_2O$ in this distance range since the shortest Cu–Cu distance (bridged through a chlorine atom) falls at 3.76 Å.

Sample Cu2.3 (dashed-line curve in Fig. 8b) is intermediate between Cu1.4 and Cu9.0, showing a first shell peak that begins to have an evident asymmetric tail in the high R region due to a small fraction of Cu–Cl contributions and exhibiting a broad component in the 2.30- to 3.50-Å region that begins to be significantly above the noise level. It is worth noticing that by Fourier filtering this broad and unresolved signal in the same range used for Cu9.0 (see the first spectrum from bottom, 10-times magnified, in Fig. 8a), we obtain a very weak $\chi(k)$ signal that has, in the 6- to 12-Å^{-1} region, the same frequency and the same relative intensity of the strong second shell extracted from Cu9.0. This result is of particular relevance since it evidences that the second shell signal of the Cu2.3 sample, although extremely weak because the fraction of copper absorbers contributing to this signal is very small, is due to the same species that generates the strong signal in sample Cu9.0. This important statement could not be assessed on the basis of a simple inspection of the FT reported in Fig. 8b.

By summarizing the EXAFS results on aged samples, we can conclude that, within the sensitivity of the technique, the first shell around Cu is due to oxygen atoms only in sample Cu1.4, while it is mainly due to oxygen atoms with a small contribution of chlorine atoms in sample Cu2.3 and is due to both O and Cl atoms in sample Cu9.0. This fact is fully demonstrated by the application of the Lee and Beni criterion (see the related discussion in Section 3.2 of Ref. (1)) as clearly evidenced in Fig. 9, where the FT corrected by the Cu–O phase is reported for the three samples. In fact, (i) for Cu1.4 the imaginary part of the FT is totally symmetric with respect to its modulus; (ii) in sample Cu2.3 only a weak asymmetry is observed; (iii) a complete asymmetry is shown for sample Cu9.0. Notice that no significant constructive second shell contribution has been observed for sample Cu1.4, while on the contrary, a strong contribution, mainly due to paratacamite, is observed in sample Cu9.0. Finally, in sample Cu2.3 only a relative small fraction of Cu atoms associated with the paratacamite is observed.

The most relevant result emerging from the whole set of presented data is that in samples with high-Cu content the main species formed is hydrated $CuCl_2$, which evolves with time toward $Cu_2(OH)_3Cl$. The presence of a copper hydroxochloride phase like paratacamite agrees well with a few previous observations reported in the literature (8–11). The conversion of copper chloride into paratacamite, which does not take place spontaneously, is likely catalyzed by surface Brønsted basic sites, as suggested by Zipelli *et al.* (9), who have observed that the transformation occurs only for $CuCl_2 \cdot 2H_2O$ supported on γ-alumina, while it is absent in the $CuCl_2 \cdot 2H_2O/\alpha$-$Al_2O_3$ system (having very few basic [OH] groups) and in $CuCl_2 \cdot 2H_2O$ supported on silica (having only acidic [OH] groups). The reaction can be schematized as follows,

$$2CuCl_2 + 3(>\text{Al–OH}) \rightarrow Cu_2(OH)_3Cl + 3(>\text{Al–Cl}), \quad [1]$$

and can be favored by the presence of water, which can take part in the reaction either directly or, more probably, indirectly, by restoring the already reacted [OH] groups. The formation of intermediate hydrolysis products has been suggested, as a mere hypothesis, by Avila *et al.* (8). As a matter of fact, the inorganic chemistry books report the existence of various basic chlorides of the general formula $Cu_2(OH)_xCl_{4-x}$, $Cu_2(OH)_3Cl$, being paratacamite the most stable (4–7). It is quite possible that the hydrolysis reaction proceeds through various steps, where the [OH] groups progressively substitute chlorine in the first coordination sphere of copper. In samples prepared following

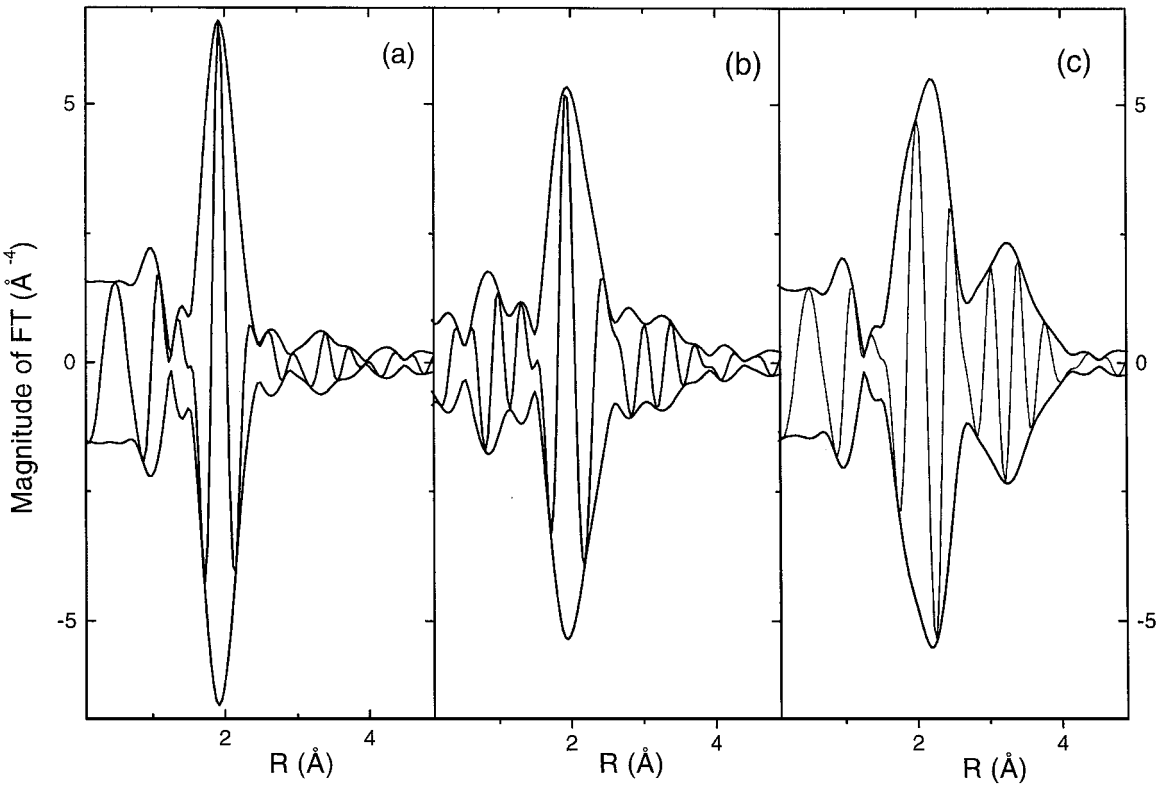

FIG. 9. Modulus and imaginary part of the k^3-weighted and Cu–O phase-corrected FT for Cu1.4, Cu2.3, and Cu9.0 samples, parts (a), (b), and (c), respectively.

the procedures described in the Experimental section of paper (1), we have found only paratacamite. However, by changing the procedure, we have observed, by XRD, the presence of other compounds. For example, when the wet sample was kept under air in an open vessel, diffraction lines corresponding to $Cu_{11}(OH)_{14}C_{l8} \cdot 6H_2O$ appear after a few hours (together with paratacamite pattern) and then disappear because of the transformation of this hydroxochloride into the more stable paratacamite. Another example concerns a sample dried at 343 K, where a hydroxochloride of the formula $Cu_3(OH)_2Cl_4 \cdot 2H_2O$ was found, together with a small quantity of paratacamite. The compound is rather stable and its transformation into paratacamite is very slow. In more general terms, let us emphasize that all the procedures involving a mild drying step followed by exposure to the atmosphere always give, as a final product, paratacamite. This consideration probably explains why, to the best of our knowledge, hydroxochlorides different from paratacamite have never been reported in the literature on oxychlorination catalysts.

Figure 10 gives an overall view of the behavior of the different samples under aging as monitored by solubility measurements. In the graph the copper solubility is reported vs the total copper concentration. The full line represents the reference, i.e., the value corresponding to a hypothetical total solubility of the copper as $CuCl_2$. Dashed, dotted, and dot–dashed lines represent the solubility data of 1-h, 1-day, and 6-months aged samples, respectively. At each abscissa value, the difference between the measured line and the reference line represents the value corresponding to the

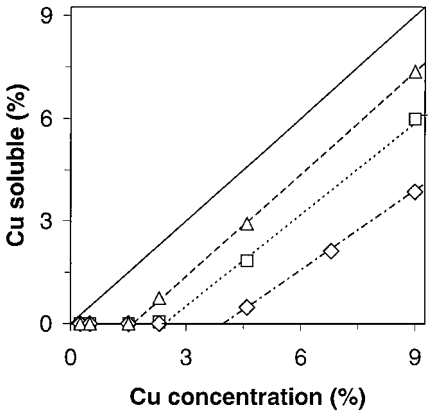

FIG. 10. Dependence of copper solubility of 1 h (Δ symbols and dashed line), 1 day (□ symbols and dotted line), and 6 months (◇ symbols and dashed–dotted line) aged samples on copper concentration pointing out the effect of copper content on copper species present on the solid. Full line represents the reference: the hypothetical 100% solubility of copper as $CuCl_2$. To verify the linearity of the reported trend for 6-month aged samples, an additional sample (Cu6.8), with Cu loading intermediate between that of Cu4.6 and Cu9.0 samples, has been added.

insoluble fraction. In freshly prepared samples, the paratacamite is formed only in a very low amount and the insoluble copper is quite completely due to the surface aluminate species. As pointed out in Ref. (1) its amount is constant (independent on the Cu concentration) and corresponds to about 1.6 wt% Cu (0.95 wt% Cu/100 m^2), which is the saturation concentration of Cu(II) hosted in octahedral sites of an γ-alumina surface for samples prepared from $CuCl_2 \cdot 2H_2O$. At each abscissa value, the difference between the solubility measured at two aging times (1 h–1 day; 1 day–6 months) gives the amount of paratacamite formed during the corresponding period. After 1 day of aging, copper chloride is almost absent in the Cu2.3 sample, but it is still present on samples of higher copper content. In the following months, the formation of paratacamite continues: however, even after 6 months, the copper chloride is not completely transformed into the hydroxochloride. This suggests that once the basic sites of alumina are consumed by HCl (formed in the chloride hydrolysis), the reaction stops or, at least, becomes much slower.

The above results allow us a first rationalization of the literature data. By a simple comparison of the Cu solubility percentage versus the total copper content of our data (Fig. 10) with those given in Refs. (8) and (12) and reported in Fig. 11a, a similar trend is observed. In fact, in both cases, a null solubility has been found on samples with low-Cu concentrations, while at higher loading, the solubility increases linearly with copper content and data lie on lines that can be considered, in a first approximation, as parallel to the reference one. On a quantitative ground, a quick inspection of the plot indicates a strong degree of irreproducibility of the solubility measurements made in the different laboratories. However, all these discrepancies are only apparent and can be interpreted on the basis of our model. In fact, two factors influence the amount of soluble copper of γ-alumina-supported $CuCl_2$: (i) the surface area of the support, which ultimately determines by the saturation amount of insoluble surface aluminate (being the saturation surface density of 0.95 wt% Cu/100 m^2) see Ref. (1)] and the aging time, which determines by the conversion of soluble copper chloride into insoluble paratacamite. If we organize the data reported in Refs. (8) and (12) (black symbols), together with our data (open symbols), on the basis of the fact that they have been obtained on supports with different areas (222 and 100 $m^2\ g^{-1}$ for Refs. (8) and (12), respectively), the resulting picture is obtained by reporting the Cu concentration normalized to the surface area of the support (Fig. 11b). In this way the only remaining free parameter is aging: from comparison with our set of data, measured at well-defined aging times, we can conclude that samples studied in Refs. (8) and (12) have been measured at an aging time intermediate between 1 day and 6 months (closer to 1 day).

All the samples from Refs. (8) and (12) having a Cu concentration higher than 0.95 wt% Cu/100 m^2 contain paratacamite. Its amount is given by the difference between the measured solubility and the values lying on the line interpolating the data obtained from freshly impregnated samples (dashed line in Fig. 11b). For each abscissa value, the dashed line gives the solubility that the authors of Refs. (8) and (12) should have obtained on freshly prepared samples. The difference between that value and the experimental ones directly gives the amount of paratacamite present in their samples at the time when the solubility measurement has been done.

3.2. *Evolution of Cu Species upon Heating*

In this section we report on the effect of heating on 6-month aged samples. As already pointed out (1), samples with low Cu content (Cu0.25, Cu0.5, and Cu1.4), i.e., samples containing only surface Cu aluminate, are not affected

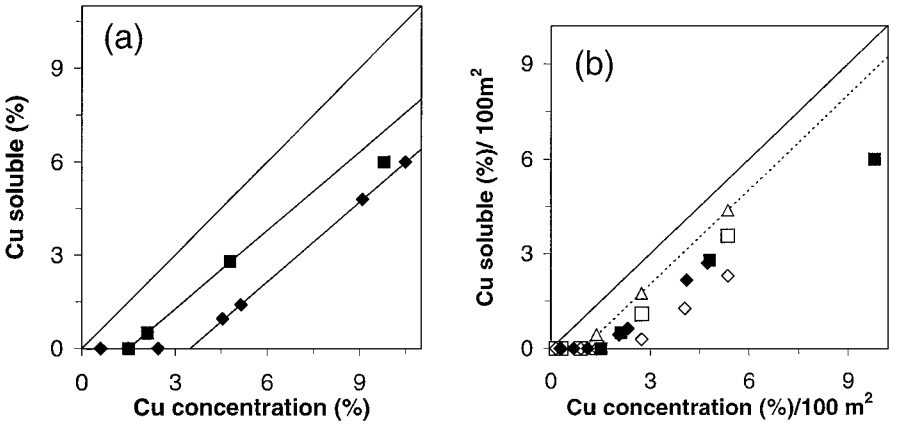

FIG. 11. Comparison of copper solubility values with literature data. Full line as in Fig. 10. Part (a): data obtained from Refs. (8) and (12). Part (b) our data (open symbols) and literature data (black symbols) summarized together by renormalizing the values to the surface area of the support. Dashed line reports the linear fit on the as-prepared samples (1-h aged) and represents the fraction of copper available once the surface aluminate has been formed, i.e., the maximum amount of soluble copper in Al_2O_3-supported $CuCl_2$.

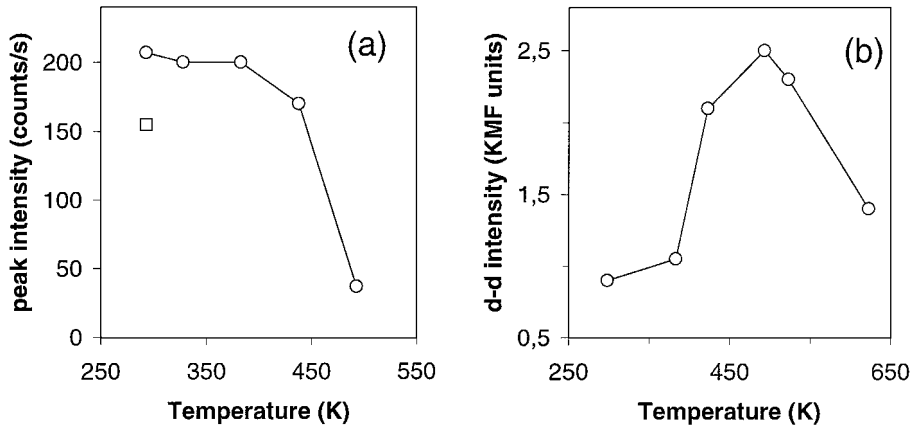

FIG. 12. Part (a): effect of heating temperature on the paratacamite 16.2° 2θ XRD peak intensity (○) for sample Cu9.0. The symbol (□) represents 16.2° 2θ XRD peak intensity of the sample heated at 500 K and kept under atmosphere for a long period. Part (b): effect of heating temperature on the intensity of the *d–d* transition band (again sample Cu9.0).

by thermal treatments, even at temperatures as high as 923 K (only a loss of Cl is observed, which does not affect the Cu species (1)). On the contrary, the samples containing Cu chloride (Cu9.0 and Cu4.6) undergo upon heating at 493 K a color change from green (the color of $CuCl_2 \cdot 2H_2O$ and of paratacamite) to brownish or brown. This is due to water removal from copper chloride: in fact, the color of anhydrous Cu chloride is brown. Surprisingly, this color change is observed also on the Cu2.3 sample, even if the solubility test has shown that almost all the copper chloride has been transformed into paratacamite (see Fig. 10), which keeps this color green, even under heating.

To understand this unexpected fact, some test experiments have been performed by heating at 423 K the mechanical mixtures of (i) alumina and paratacamite and (ii) alumina impregnated with HCl and paratacamite. The copper content (9.0 wt%) is the same for both mixtures. The total chlorine content (25% coming from paratacamite and 75% coming from HCl) in the second mixture is the same that of the Cu9.0 sample. We have found that the mechanical mixture of pure alumina and paratacamite does not change color under heating (the same holds for pure paratacamite). On the contrary the color of the mixture containing chlorinated alumina turns to the brown color, typical of anhydrous copper chloride. The brown color was kept unchanged when the sample was preserved under a dry atmosphere. On the contrary, it quickly turns to green in the presence of moisture. From these two tests we conclude that (i) at 423 K, alumina impregnated with HCl looses part of the acid under heating and (ii) paratacamite reacts with HCl released from the alumina phase to form anhydrous copper chloride. Based on this evidence, we can conclude that the surface $>$Al–Cl species, initially present on our samples because of the formation of the surface aluminate (see Eq. [2] in Ref. (1)) and because of the formation of paratacamite under aging (see Eq. [1] in this work), are able to release chlorine under heating, so furnishing the amount of Cl sufficient to reverse conversion of $CuCl_2$ into paratacamite. This conclusion is confirmed by XRD measurements, performed on the Cu9.0 sample during the heating from RT to 493 K and subsequent aging at RT. The results are shown in Fig. 12a, where the dependence of the intensity of the 16.2° 2θ diffraction line of paratacamite is reported as a function of heating temperature and subsequent re-aging. It can be noted that paratacamite starts to disappear at a temperature comprised between 383 and 438 K and that it approaches the completion at 493 K. Re-exposure of samples heated to 500 K to a wet atmosphere (few months) allows the rather complete restoration of paratacamite, as demonstrated by the 16.2° 2θ diffraction line intensity of paratacamite (□ symbol in Fig. 12a). Only heating treatments above 500 K cause an irreversible decomposition of paratacamite (likely with chlorine release), which is not restored by re-exposure to moist air. By the way, this result suggests a method for more precise determination of both copper chloride and surface aluminate: solubility tests should be in fact performed on samples heated at about 500 K and cooled under a dry atmosphere (because they are paratacamite-free).

Further proof that copper chloride is restored upon heating is obtained by means of UV–Vis DRS on the Cu4.6 sample heated at various temperatures and re-exposed to air for a short time (2 h: sufficient to re-hydrate the chloride but avoiding hydrolysis). The results, shown in Fig. 12b, point out an increase of the *d–d* transition intensity up to 523 K (chloride formation), followed by a sharp decrease at temperatures higher than 623 K (chloride decomposition). Although this result can not be regarded as quantitative, it nevertheless confirms the above-reported conclusion.

Thermal activation implies a loss of the resolution of the hyperfine signal of EPR spectra (bottom spectrum in Fig. 5), progressively appeared upon aging up to 6 months (second

spectrum from the bottom in Fig. 5). This experimental evidence reflects the evolution from a Cu(II) environment with long-range ordering (crystalline paratacamite) to a highly heterogeneous one (amorphous, highly dispersed, anhydrous $CuCl_2$).

As final proof of the restoration of anhydrous $CuCl_2$ after heating, we will now report the structural information on the local environment of copper obtained from EXAFS data. The upper curve in Fig. 13a represents the averaged k-weighted $\chi(k)$ function of the Cu9.0 sample measured at RT *in vacuo* after aging and heating. The so-obtained $k\chi(k)$ function is very different from that obtained before heating (third spectrum from the top in Fig. 8a). The k^3-weighted, phase-uncorrected, FT function, calculated over the 2.69- to 12.27- $Å^{-1}$ range ($\Delta k = 9.58$ $Å^{-1}$), gives only one peak at 1.81 Å, as shown in the full-line curve of Fig. 13b. The comparison with the FT function of the sample before heating (dotted curve in Fig. 13b) indicates a dramatic modification of the local environment of copper: in the first shell, we observe the nearly total disappearance of the Cu–O contribution (mainly due to the oxygen of paratacamite at 1.93 Å), while in the higher R region we note the total erosion of the prominent and complex second shell contribution previously attributed to paratacamite (see section 3.1). The disappearance of the paratacamite, evidenced by XRD, is so confirmed at the local level.

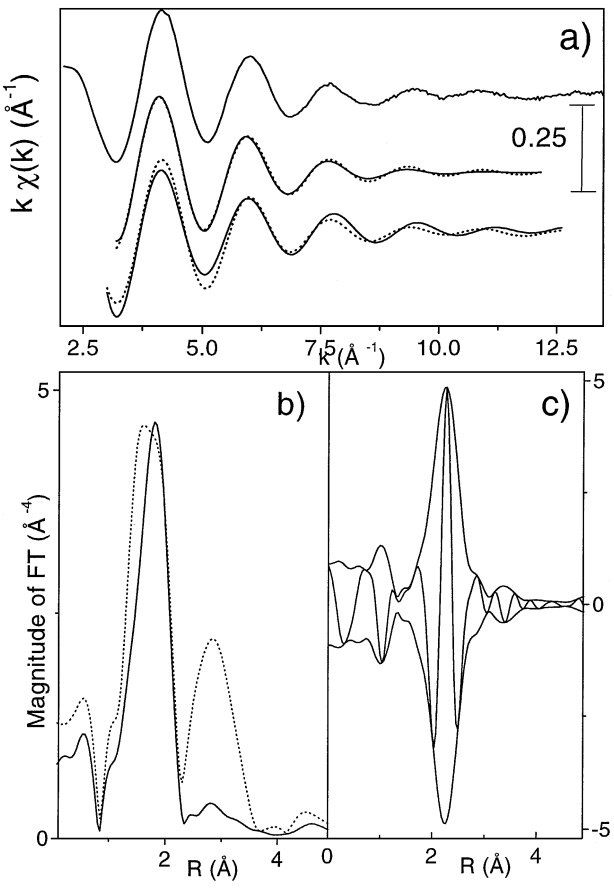

FIG. 13. EXAFS study on sample Cu9.0 after aging and heating. Part (a): raw EXAFS data (upper curve), first shell filtered $\chi(k)$, and comparison with best fit obtained using Cu–Cl (middle curves) and Cu–O (lower curves) models, respectively. Part (b) k^3-weighted, phase-uncorrected FT for Cu9.0 after 6 months of aging and subsequent heating, dotted and full lines, respectively. Part (c) modulus and imaginary part of the k^3-weighted and Cu–Cl phase-corrected FT for sample Cu9.0 after aging and heating.

The first shell contribution was then filtered in the 0.84- to 2.37-$Å^{-1}$ range ($\Delta r = 1.53$ Å) and modeled as chlorine atoms coordinated to Cu ions in the nearest local shell imposed by the structure of anhydrous $CuCl_2$ (13): $N = 4$ chlorine atoms at 2.26 Å. The quality of the fit can be appreciated in the middle curves reported in Fig. 13a (dotted and full lines for experimental and fit, respectively). McKale phases and amplitudes (14) have been adopted. The agreement between experimental and fit is particularly good if we consider that only three parameters (ΔE, the Debye–Waller factor and the electron mean-free path parameter) were optimized. In no cases the experimental signal could be reproduced by using Cu–O phases and amplitudes extracted from CuO, as documented by the four parameter fit reported in the bottom spectra of Fig. 13a. This clearly indicates that, after heating, anhydrous $CuCl_2$ has been formed. The high first shell Cu–Cl Debye–Waller factor ($\sigma = 0.12 \pm 0.02$ Å) obtained from the fit indicates a high disorder, probably of static origin. Moreover, the absence of any significant higher shell contribution indicates that, at higher distance, the static disorder is even greater: this observation is of paramount relevance since it is direct proof of the absence of long-range ordering in the anhydrous phase and consequently explains the absence of any $CuCl_2$ line in XRPD patterns.

As a final remark, we point out that chlorine is not the sole scatterer around copper because the phase-corrected FT has an imaginary part which is not totally symmetrical with respect to its modulus (see Fig. 13c). This is not surprising since we well know now that this sample contains a small fraction (1.5 wt%) of stable surface aluminate, where Cu is surrounded by about 5 oxygen scatterers at about 1.92 Å (1).

As a result of the whole experimental data described in this work, we have obtained a clear picture describing the evolution followed by copper species formed on high Cu concentration samples under the effect of both aging and heating. Freshly prepared samples contain copper chloride, and aging causes its progressive conversion into paratacamite, while heating moves back the equilibrium between the two species in favor of $CuCl_2$.

We have observed that experimental conditions can deeply affect the quantitative aspects of the heating process. If the conditions are not appropriate, a loss of a fraction of Cl atoms released by the surface during heating will give rise

to an only partial recovery of the initial conditions and to the formation of copper compounds with a Cl/Cu atomic ratio intermediate between 0.5 (paratacamite) and 2 (copper chloride). It is however worth noticing that this process has a relatively high efficiency, as demonstrated by the fact that we have been able to repeat a few times the aging/heating cycle obtaining every time the color changes.

Few authors report results obtained on heated samples (8–11, 15), indicating the presence of paratacamite (detected by XRD) on samples treated in air in the 383–573 K range. This presence can be due either to a poor rechlorination efficiency in the heating procedures followed by the authors, to a subsequent hydrolysis process due to re-aging, or to both effects. Among the quoted papers, only Zipelli *et al.* (9) have studied the sample both before and after thermal activation, being so able to give some information on the relative change that the sample had undergone during the treatment. However, they did not take into account the reverse transformation of paratacamite into copper chloride. Following the discussion reported at the end of section 3.1, we can conclude that data concerning heated samples can be misleading if no information is given on the time elapsed between heating and measurements.

Obviously, in the oxychlorination reaction environment, both the presence of HCl and the high temperature (490–530 K) strongly favor the $CuCl_2$ phase with respect to paratacamite. A significant amount of paratacamite cannot be present in the reaction environment, and thus cannot be either the active component of the catalyst or responsible for its decay. So, the presence of paratacamite, found by us together with several authors on alumina-supported copper chloride samples, must be considered uninfluential under the catalytic point of view. In other words, the investigation on RT samples is not enough to obtain a realistic picture of the alumina-supported copper chloride catalyst. We can so conclude this paragraph by affirming that the only copper species present when the reaction starts (i.e., before the contact with reagents) are the surface aluminate and a highly dispersed anhydrous $CuCl_2$. Stimulated by this conclusion, in the next paragraph, we report the results of activity tests aimed to establish the role played by these two species in the activity of the catalyst.

3.3. Role of Copper Species in the Oxychlorination Reaction

To explore the reaction mechanism, we have performed depletion tests, where ethylene is sent on the sample in the absence of HCl reactant (see Experimental section). In such a way, the only chlorine source available for the C_2H_4 conversion into $C_2H_4Cl_2$, is on the catalyst itself: i.e., both Cl present in dispersed Cu species and on the surface of the support (1). The total ethylene conversion obtained on Cu9.0, Cu4.6, and Cu1.4 catalysts and on bare γ-alumina

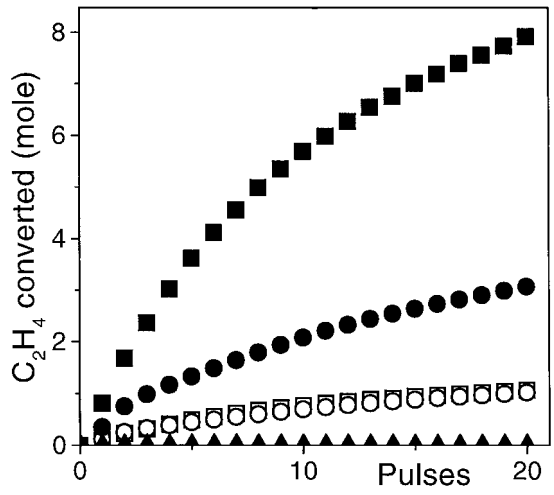

FIG. 14. Ethylene conversion to 1,2-dichloroethane vs the number of pulses on 9.0, 4.6, and 1.4 wt% samples: (black ■, ●, and ▲ symbols, respectively). Points of bare γ-Al_2O_3 overlaps those of the Cu1.4 sample. Open symbols □ and ○ refer to 9.0 and 4.6 wt% loaded samples normalized by "active" Cu concentration (see text).

support are reported in Fig. 14 (full-black symbols) as a function of the number of pulses. We observe that only catalysts containing $CuCl_2$ are active, while both bare γ-alumina and Cu1.4 catalysts have null activity. As expected, the activity per pulse of both Cu9.0 and Cu4.6 is reduced by increasing the number of pulses due to the progressive consumption of chlorine. It is however worth noticing that catalyst Cu9.0 is still active even after 35 pulses (points not reported in Fig. 14): at this stage, the integrated chlorine consumption is equivalent to 74% of the total available amount calculated in the following reaction:

$$2CuCl_2 + C_2H_4 \rightarrow 2CuCl + C_2H_4Cl_2. \qquad [2]$$

This means that the chlorine atoms of $CuCl_2$ must be the main chlorine source in the reaction since the small fraction of Cl-forming surface >Al–Cl species cannot explain a so high $C_2H_4Cl_2$ formation. It is also evident that ethylene is able to use most (probably all) of the chlorine of $CuCl_2$, so confirming that copper chloride must be in an extreme dispersed form. This catalytic result is thus in agreement with the absence of both $CuCl_2$ diffraction lines in XRD measurements and of second shell contributions in the EXAFS data. Finally, it is worth noticing that the increment of conversion measured by moving from a Cu4.6 to Cu9.0 catalyst is more than directly proportional to the increment of copper. This fact is not surprising since we have demonstrated that the fraction of Cu forming the surface aluminate (1.6 wt% Cu for our support having 168 $m^2\ g^{-1}$) is inactive: this means that the fraction of active copper species in samples Cu4.6 to Cu9.0 is only 3.1 and 7.5 wt% Cu, respectively. By re-plotting the activity curves of samples Cu4.6 to Cu9.0 renormalized by factors 1/3.1 and 1/7.5,

we see that they overlap rather well (see Fig. 14 (open symbols)), giving further proof of the validity of our model.

4. CONCLUSIONS

The surface structures formed upon alumina impregnation with copper chloride depend on both copper concentration and sample "history". At copper content lower than 0.95 wt% Cu/100 m^2 of support, the Cu is present as a surface aluminate, which is stable under both aging and heating treatments. At higher loadings copper chloride precipitates directly from the solution during the drying process, with the formation of $CuCl_2 \cdot 2H_2O$. Cu chloride undergoes a slow hydrolysis with the formation of various insoluble copper hydroxochlorides, whose structure is mainly depending on drying conditions. The final product of hydrolysis is crystalline paratacamite. The HCl released during the hydrolysis reacts with alumina with the formation of >Al–Cl species. Under heating, the alumina partially releases the chlorine fixed to the surface with the transformation of paratacamite into copper chloride. In the oxychlorination reaction conditions paratacamite is absent and only surface aluminate and copper chloride (or products arising from the interaction of these compounds with reactants or reaction products) are present on the catalyst. It has been demonstrated that surface aluminate is not active and that the active phase is $CuCl_2$.

ACKNOWLEDGMENTS

We are strongly indebted to G. Vlaic (Sincrotrone Trieste and Dipartimento di Chimica Università di Trieste), F. Geobaldo (Politecnico di Torino), and F. Villain (LURE), for their relevant and friendly support during EXAFS measurements, to G. Turnes Palomino (Dipartimento di Chimica IFM Università di Torino) for EPR measurements, to E. Giamello (Dipartimento di Chimica IFM Università di Torino) for enlightening contribution in the discussion of the EPR data, and to B. Cremaschi (EVC, Porto Marghera) for her analytical support.

REFERENCES

1. Leofanti, G., Padovan, M., Garilli, M., Carmello, D., Zecchina, A., Spoto, G., Bordiga, S., Turnes Palomino, G., and Lamberti, C., *J. Catal.* **189**, 91 (2000).
2. Engberg, A., *Acta Chim. Scand.* **24**, 3510 (1970).
3. Fleet, M. E., *Acta Crystallogy B* **31**, 183 (1975).
4. Pascal, P., "Nouveau traité de chimie minérale." (Mason et c. Ed.), Paris, III, 1957.
5. Mellor, J. W., "A Comprehensive Treatise on Inorganic and Teoretical Chemistry." Longmans, Green and Co., London, 1956.
6. Sneed, M. C., Maynard, J. L., and Brasted, R. C., "Comprehensive Inorganic Chemistry," Vol. 2. D. Van Nostrand Company, New York, 1954.
7. Ball, M. C., and Coultard, R. F. M., *J. Chem. Soc. A*, 1417 (1968).
8. Avila, P., Blanco, J., Garcia-Fierro, J. L., Mendioroz, S., and Soria, J. *Stud. Surf. Sci. Catal.* **7B**, 1031 (1981).
9. Zipelli, G., Bart, J. C., Petrini, G., Galvagno, S., and Cimino, C., *Z. Anorg. Allg. Chem.* **502**, 199 (1983).
10. Solomonik, I. G., Kurlyandskaya, I. I., Ashavskaya, G. A., and Yakerson V. I., *Izv. Akad. Nauk. SSSR Ser. Khim.* **4**, 766 (1986).
11. Solomonik, I. G., Kurlyandskaya, I. I., Yakerson V. I., Kudryavtseva, T. F., Ashavskaya, G. A., Frid, M. R., Treger, Yu. A., and Sonin, E. V., *Izv. Akad. Nauk. SSSR Ser. Khim.* **11**, 2431 (1984).
12. Fortini, E. M., Garcia, C. L., and Resasco, D. E., *J. Catal.* **99**, 12 (1986).
13. Burns, P. G., and Hawthorne, F. C., *Am. Mineral.* **78**, 187 (1993).
14. McKale, A. G., Veal, B. W., Paulikas, A. P., Chan, S. K., and Knapp. G. S., *J. Am. Chem. Soc.* **110**, 3763 (1988).
15. Sermon, P. A., Rollins, K., Reyes, P. N., Lawrence, S. A., Martin Luengo, M. A., and Davies, M. J., *J. Chem. Soc., Faraday Trans. 1* **83**, 1347 (1987).